第 25 卷第 12 期 半 导 体 学 报 Vol. 25, No. 12
2004 年 12 月 CHINESE JOURNAL OF SEMICONDUCTORS Dec., 2004

# Gate-Capacitance-Shift Approach and Compact Modeling for Quantum Mechanical Effects in Poly-Gates*

Zhang Dawei[1], Zhang Hao[2], Tian Lilin[1] and Yu Zhiping[1]

(1 *Institute of Microelectronics, Tsinghua University, Beijing* 100084, *China*)
(2 *Department of Electronics and Engineering, Tsinghua University, Beijing* 100084, *China*)

**Abstract**: A new approach, gate-capacitance-shift (GCS) approach, is described for compact modeling. This approach is piecewise for various physical effects and comprises the gate-bias-dependent nature of corrections in the nanoscale regime. Additionally, an approximate-analytical solution to the quantum mechanical (QM) effects in polysilicon (poly)-gates is obtained based on the density gradient model. It is then combined with the GCS approach to develop a compact model for these effects. The model results tally well with numerical simulation. Both the model results and simulation results indicate that the QM effects in poly-gates of nanoscale MOSFETs are non-negligible and have an opposite influence on the device characteristics as the poly-depletion (PD) effects do.

**Key words**: compact model; nanoscale regime; GCS approach; QM effects in poly-gates
**PACC**: 7340Q; 6185; 0300
**CLC number**: TN304.02 **Document code**: A **Article ID**: 0253-4177(2004)12-1599-07

## 1 Introduction

With CMOS technology aggressively scaled down into the 100nm regime quantum mechnical (QM) effects in various regions of a MOSFET will be evident[1~3] and have significant influence on device characteristics. Therefore, compact models of the QM effects both in channels and poly-gates need to be established for circuit designers. However, the conventional TVS approach for compact modeling, which has been successfully utilized in the well-known SPICE model BSIM[4], is ineffective in the nanoscale regime due to the gate-bias-dependent nature of the physical effects. In this paper. a newly developed approach for compact modeling, the gate-copacitance-shift (GCS) approach, is described. It expresses the idea that the gate-bias-dependent nature may be modeled by a gate capacitance shift in addition to the threshold voltage shift.

Furthermore, although there is research on the QM effects in poly-gates based upon numerical simulations[5], compact modeling for them is absent. In this paper, based on the DG formulation[6], an analytical solution to the QM effects in poly-gates is obtained. It is then combined with the GCS approach to establish a compact model. Compared to numerical results, this model is satisfactory using different device parameters. It is concluded that the QM effects have an opposite influence on threshold voltage as the poly-depletion(PD) effects do

* Project supported by National High Technology R&D Program of China(No. 2003AA1Z1370)

Zhang Dawei male, was born in 1980, master candidate. His major interest is compact modeling for novel physical effects in nanoscaled devices.

Zhang Hao male, was born in 1983, undergraduate student. His major interest is analytical modeling for quantum mechanical effects in sub-100nm MOSFETs.

Received 18 February 2004, revised manuscript received 5 July 2004 ©2004 The Chinese Institute of Electronics

and they become more acute when the poly doping increaseswhile the PD effects behave oppositely.

## 2 GCS approach for compact modeling

In long channel MOSFETs, where the oxide layer is thick and the channel doping is light and uniform, there is no need to consider any correction to a charge model. Therefore, in the strong inversion condition, the surface charge density is expressed in the following way:

$$Q_{inv_ini} = C_{ox}(V_g - V_{th}) \quad (1)$$

with $Q_{inv_ini}$ surface charge density of inversion layer, $C_{ox}$ gate capacitance, $V_g$ gate bias, and $V_{th}$ threshold voltage. With the gate length scaled down, corrections due to various physical phenomena, e. g. short channel effects (SCEs) and drain induced barrier lowering effects (DIBL), are made with the threshold-voltage-shift(TVS) approach as is done in BSIM 4[4]. The idea of attributing all physical concerns to a $V_{th}$ shift, however, is insufficient for some physical effects in the nanoscale regime, which have gate-bias-dependence.

To demonstrate the necessity of establishing gate-bias-dependent corrections, quantum simulations are executed using DESSIS in ISE 8.0[7]. Extensive explanations for numerical simulations in this work are presented in Appendix A. In Fig. 1, the surface charge densities of the inversion layer with the poly-gate doping $N_{poly} = 3\times10^{20}cm^{-3}$, the substrate doping $N_{sub} = 10^{18}cm^{-3}$ and the gate oxide thickness $t_{ox} = 1.2\times10^{-7}cm$ are shown. The results are obtained with the classical simulation in the substrate without PD effects in the gate considered, the quantum simulation in the substrate without PD effects in the gate considered, the quantum simulation in the substrate with the inclusion of PD effects in the gate, and the quantum simulation both in the substrate and in the poly-gate. As is seen in Fig. 1, with the inclusion of the QM in the substrate, the PD in the poly-gate or the QM in the poly-gate, it is clear that the slope of the curve, i.

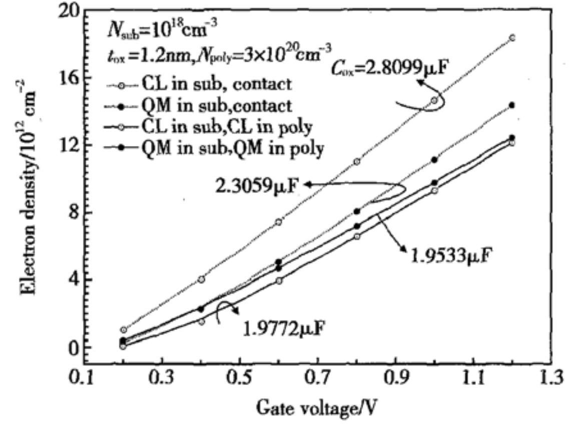


Fig. 1 Electron density, with either QM or classical (CL) effects in both substrate (sub) and poly-gate region, with $N_{poly} = 3\times10^{20}cm^{-3}$, $N_{sub} = 10^{18}cm^{-3}$, and $t_{ox} = 1.2nm$ The effective capacitances are labeled. Dashed lines represent results without the poly-gate region (contact). Solid lines represent results with the poly-gate region (poly).

e. the effective gate capacitance, has shifted. This reflects the linear dependence on the gate bias of the corrections due to these effects. Furthermore, for some of these effects, e. g. QM effects in poly-gates, the slope of the curve alters with the gate bias, which reflects the gate-bias-dependence nature of higher orders (higher than linear dependence). Proceeding from this concept, the GCS approach is formulated:

$$Q_{inv} = (C_{ox} + \Delta C_{ox})(V_g - V_{th} - \Delta V_{th}) \quad (2)$$

$$\Delta C_{ox} = \Delta C_{ox}^0 + \Delta C_{ox}^1 V_g + \Delta C_{ox}^2 V_g^2 + \cdots \quad (3)$$

$$\Delta V_{th} = \Delta V_{th}^0 + \Delta V_{th}^1 V_g + \Delta V_{th}^2 V_g^2 + \cdots \quad (4)$$

with $\Delta C_{ox}$ and $\Delta V_{th}$ the oxide capacitance shift and threshold voltage shift that may depend on $V_g$ and are expressed as the Taylor Series of $V_g$ with $\Delta C_{ox}^i$ and $\Delta V_{th}^i$, coefficients of the $i$th order. If only the 0th order, $\Delta C_{ox}^0$, is kept, the correction is linearly dependent on gate bias supposing the correction is defined as $Q_{inv} - Q_{inv_ini}$. However, the QM effects in poly-gates need higher ordered corrections and therefore $\Delta C_{ox}^1$ is needed, which is shown in the next section.

The GCS approach is piecewise for various physical effects. It comprises the gate-bias-dependent nature of corrections in the decanano-scaled

regime and has a straightforward relation with gate bias. The relation of these effects to device parameters is reflected in the coefficients. In the following sections, it is applied for the purpose of developing a compact model for the QM effects in poly-gates on the basis of DG formulation.

## 3 Quantum mechanical effects in poly-gate region

The well-established DG method is the lowest order approximation of the Wigner function approach to including QM effects in carrier transport[6]. The essential formulation of the DG method is to include an additional quantum potential into the Boltzmann statistics of as follows (take electrons as example):

$$n = n_i \exp[q(\Psi + \Delta\Psi_{QM} - \phi_n)/k_B T] \tag{5}$$

$$\Delta\Psi_{QM} = \frac{2}{\sqrt{n}} \times \nabla \times \left(\frac{\hbar^2}{4lqm_n^*} \nabla\sqrt{n}\right) \tag{6}$$

where $n$ electron density, $n_i$ intrinsic carrier density, $\Psi$ electric potential, $\Delta\Psi_{QM}$ quantum potential, $\phi_n$ electron quasi-Fermi level, $k_B$ Boltzmann constant, $T$ temperature, $l$ space dimensionality ($l = 3$) and $m_n^*$ effective mass for electron. In Fig. 2, the potential distribution and electron distribution in the poly-gate region of a MOS structure are shown, obtained from numerical simulations that are executed throughout the three regions of the MOS structure (explained in Appendix A). The poly-gate is uniformly doped. The "hill-like" non-uniform distribution of electrons unmistakably demonstrates the QM effects because it reflects the wave nature of electrons and the boundary conditions required by Poisson equation and Schrödinger equation[5]. The QM effects substantially alter the potential distribution from the classical case and need to be modeled. The rest of this section introduces an approach to compact modeling the QM effects in poly-gates.

Starting from the DG formulation in Eqs. (5), (6), $\Delta\Psi_{QM}$ is related to $\Psi$ in the following manner (specific deduction is carried out in Appendix B):

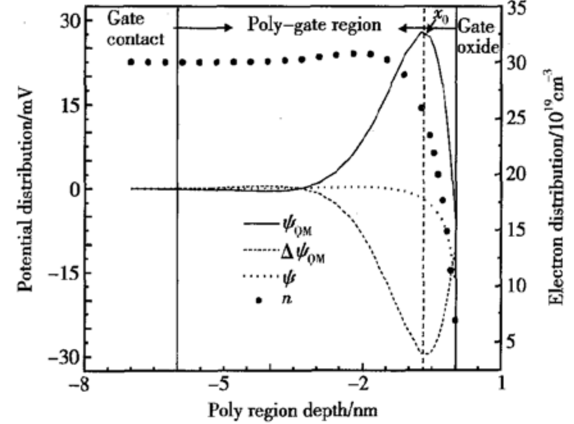


Fig. 2 Potential distribution, quantum potential distribution and electron distribution in poly-gate with $N_{poly} = 10^{20}\,cm^{-3}$, $N_{sub} = 10^{18}\,cm^{-3}$, and $t_{ox} = 1.2nm$ Solid line stands for potential, dash line stands for quantum potential, and solid dots stands for electron. The reference origin of the coordinate is the poly-gate/gate-oxide interface, with to the left the poly-gate region and to the right the gate-oxide.

$$\frac{\hbar^2}{4lm_n^* k_B T} \times \frac{\partial^2 \Delta\Psi_{QM}}{\partial x^2} + \left(\frac{\hbar^2 q}{4lm_n^* k_B^2 T^2} \times \frac{\partial\Psi}{\partial x}\right)\frac{\partial\Delta\Psi_{QM}}{\partial x} - \Delta\Psi_{QM} + \frac{\hbar^2 q}{8lm_n^* k_B^2 T^2} \times \left(\frac{\partial\Psi}{\partial x}\right)^2 + \frac{\hbar^2}{4lm_n^* k_B T} \times \frac{\partial^2\Psi}{\partial x^2} = 0 \tag{7}$$

Due to the highly non-linear relations among $n$, $\Psi$, and $\Delta\Psi_{QM}$, (see Eqs. (5), (6), and Poisson equation) which lead to the non-linearity of Eq. (7), it is difficult to find the analytical solution to $\Delta\Psi_{QM}$. Thus, the following simplification is made which to some degree decouples Eqs. (5) and (6) and makes it possible to determine analytical solution:

$$\Delta\Psi_{QM} = \frac{\hbar^2}{2lqm_n^* \sqrt{n_{cl}}} \times \frac{\partial^2 \sqrt{n_{cl}}}{\partial x^2} \tag{8}$$

where $n_{cl}$ is the classical electron distribution. The error due to this simplification is compensated by parameters $c_1$ and $c_2$, introduced at the end of this section. Then, with Eqs. (6) and (8), Equation (5) is substituted into the Poisson equation with the approximation $e^u \approx 1 + u$, and the following differential equation for the electric potential results:

$$\left(\frac{\hbar^2}{4lm_n^* k_B T} - \frac{\epsilon_{Si} k_B T}{q^2 N_p}\right)\frac{\partial^2\Psi}{\partial x^2} + \frac{\hbar^2 q}{8lm_n^* k_B^2 T^2}\left(\frac{\partial\Psi}{\partial x}\right)^2 + \Psi = 0 \tag{9}$$

With the gate contact as the potential reference and the boundary conditions $\frac{\partial\psi}{\partial x}\Big|_{x=0} = \frac{\epsilon_{ox}}{\epsilon_{Si}}E_{ox}$, $\frac{\partial\psi}{\partial x}\Big|_{x=x_0} = 0$ with $E_{ox}$ electric field in the oxide layer at the poly-gate/gate-oxide interface, the potential profile at right side of $x_0$ (shown in Fig. 2) is determined from Eq. (9):

$$\psi(x) = a\left[x + \frac{\epsilon_{ox}}{2\epsilon_{Si}a}\times E_{ox}\right]^2 + b \qquad (10)$$

with $a = -\frac{2lk_B^2T^2m_n^*}{\hbar^2 q}$, and $b = \frac{k_BT}{q} - \frac{4lm_n^*(k_BT)^3\epsilon_{Si}}{\hbar^2q^3N_p}$. Therefore, in the quantum case, the voltage drop in poly-gates, $V_{poly}$, equals $-\frac{\epsilon_{ox}^2}{4a\epsilon_{Si}^2}\times E_{ox}^2 - b$. The relation between $E_{ox}$ to $V_g$ is straightforward and $V_{poly}$ is obtained with the following expression:

$$V_{poly} = -\frac{C_{ox}^2}{4a\epsilon_{Si}^2}\times(V_g - V_{FB} - V_S + b)^2 - b \qquad (11)$$

with $V_{FB}$ flat-band voltage and $V_S$ surface potential in the substrate. With Eq. (11), $\Delta C_{ox}^1$, $\Delta C_{ox}^0$, and $\Delta V_{th}^0$ are determined by the following equality:

$$(C_{ox} + \Delta C_{ox}^1V_g + \Delta C_{ox}^0)(V_g - V_{th} - \Delta V_{th}^0) = C_{ox}(V_g - V_{th} - V_{poly}) \qquad (12)$$

Therefore, $\Delta C_{ox}^1$, $\Delta C_{ox}^0$, and $\Delta V_{th}^0$ are obtained:

$$\Delta C_{ox}^1 = \frac{C_{ox}^3}{4a\epsilon_{Si}^2} \qquad (13)$$

$$\Delta V_{th}^0 = -\left[\frac{C_{ox}^2}{4a\epsilon_{Si}^2}\times(b - V_S - V_{FB})^2 + b + \frac{V_{th}}{C_{ox}}\right]\Big/\left[1 + \frac{1}{C_{ox}}\right] \qquad (14)$$

$$\Delta C_{ox}^0 = \frac{C_{ox}^3}{2a\epsilon_{Si}^2}\times\left[b - V_S - V_{FB} + \frac{V_{th}}{2}\right] \qquad (15)$$

As is shown, $\Delta C_{ox}^0$ and $\Delta C_{ox}^1$ reflect the gate-bias-dependence nature of the QM effects in poly-gates. The compact modeling for the QM effects in poly-gates based on the GCS approach has been generally established. However, due to the simplifications made in Eq. (8), $a$ and $b$ are not adequately precise although they are roughly correct in terms of the order. In Fig. 3, the potential distributions with different $N_{sub}$, $N_{poly}$, and $t_{ox}$ are shown. It is conclusively demonstrated that $a$ and $b$ change with device parameters. Therefore, in this compact model, they are replaced by $a'$ and $b'$ where $a' = c_1\times a$ and $b' = c_2\times b$, and the relationship between them and

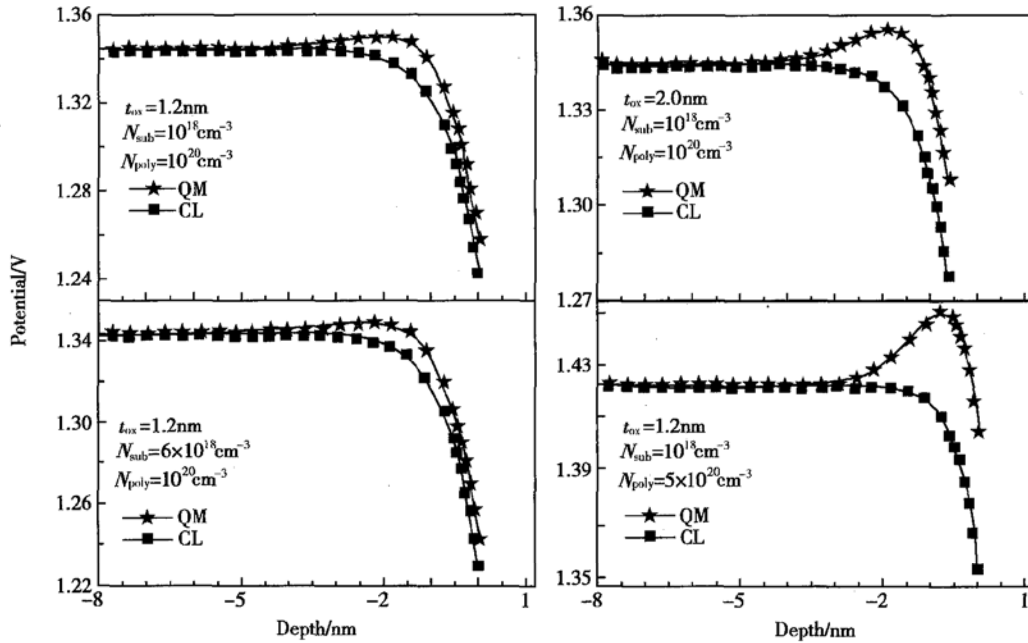


Fig. 3 Potential distribution, with different poly-gate doping, substrate doping, and oxide ($N_{poly} = 10^{20}$ cm$^{-3}$, $N_{poly} = 5\times10^{20}$cm$^{-3}$; $N_{sub} = 10^{18}$cm$^{-3}$, $N_{sub} = 6\times10^{18}$cm$^{-3}$; $t_{ox} = 1.2\times10^{-7}$cm, $t_{ox} = 2\times10^{-7}$cm) at a gate bias $V_g = 0.8$V The reference origin of the coordinate is the poly-gate/gate-oxide interface, with the poly-gate region to the left and the gate-oxide to the right.

the device parameters should be determined. The relation between the acuteness of the QM effects to $N_{sub}$ is weak as is shown in Fig. 4 (see numerical results), for the curves with different $N_{sub}$ have almost the same slopes, indicating the same acuteness of the QM effects. On the other hand, the acuteness of the QM effects is strongly dependent

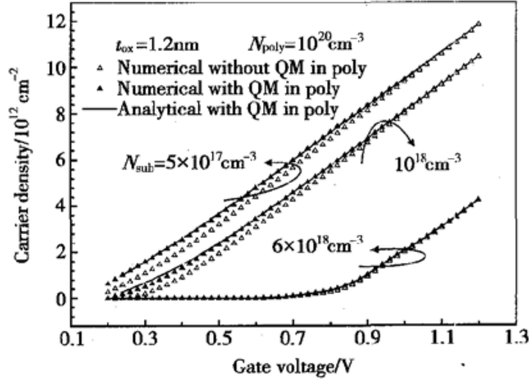


Fig. 4　Carrier density, with $t_{ox}$ = 1.2nm, $N_{poly}$ = $10^{20}$ cm$^{-3}$ and different substrate doping ($N_{sub}$ = 5 × $10^{17}$ cm$^{-3}$, $N_{sub}$ = $10^{18}$ cm$^{-3}$ and $N_{sub}$ = 6 × $10^{18}$ cm$^{-3}$)　Solid symbols represent numerical results with QM in the poly-gate and hollow symbols represent those without QM in the poly-gate. Solid lines stand for analytical results with QM in the poly-gate.

on $N_{poly}$ and $t_{ox}$, as is shown in Figs. 6 and 7 (see numerical results). Therefore, the following relationships between $c_1$, $c_2$ and $N_{poly}$, $t_{ox}$ are developed:

$$c_1 = \left[0.7962 + 1.2307 \times 10^{22} \times \left(\frac{N_{poly}}{n_i}\right)^{-2.3254}\right] \times \left[0.00109 + 0.04653 \times e^{-t_{ox}/0.54133}\right] \quad (16)$$

$$c_2 = (0.3971 + 0.4964 \times t_{ox}) \times \left[-87.0793 + 6.777 \times \lg\left(\frac{N_{poly}}{n_i}\right) - 0.12599 \times \left[\lg\left(\frac{N_{poly}}{n_i}\right)\right]^2\right] \quad (17)$$

with $N_{poly}$ and $n_i$ in dimensions [$10^{20}$cm$^{-3}$], and $t_{ox}$ in [nm]. With Eqs. (16) and (17), the compact model for the QM effects in poly-gates has been completely developed. In Fig. 5, the relation of $\Delta V_{th}^0$ to $N_{poly}$ is presented, which clearly indicates the heavier the poly doping, the more acute the QM effects are. The analytical results are then compared to the

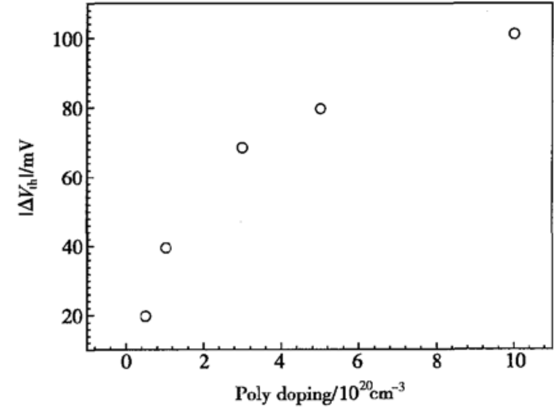


Fig. 5　Threshold voltage shift versus poly-gate doping, with $N_{sub}$ = $10^{18}$cm$^{-3}$ and $t_{ox}$ = 1.2nm.

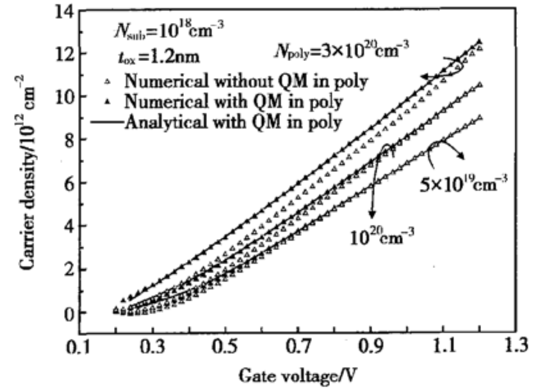


Fig. 6　Carrier density, with $t_{ox}$ = 1.2nm, $N_{sub}$ = $10^{18}$ cm$^{-3}$ and different poly-gate doping ($N_{poly}$ = 5 × $10^{19}$ cm$^{-3}$, $N_{poly}$ = $10^{20}$ cm$^{-3}$, and $N_{poly}$ = 3 × $10^{20}$ cm$^{-3}$) Solid symbols represent numerical results with QM in the poly-gate and hollow symbols represent those without QM in the poly-gate. Solid lines stand for analytical results with QM in the poly-gate.

numerical results (the explanation for how to obtain the numerical results are given in Appendix A) with different $N_{sub}$, $N_{poly}$, and $t_{ox}$, shown respectively in Figs. 4, 6, and 7. The numerical results without the QM effects considered in poly-gates are also shown. It is concluded that: (1) this model has satisfactory accuracy with an average relative error below 3%; (2) the QM effects are non-negligible in nanoscale MOSFETs where channel doping is heavy and gate-oxides are ultra-thin; (3) the QM effects result in a gate-capacitance shift, linearly dependent on gate bias; (4) the QM effects result

in a threshold voltage reduction and therefore behave oppositely as the PD effects do.

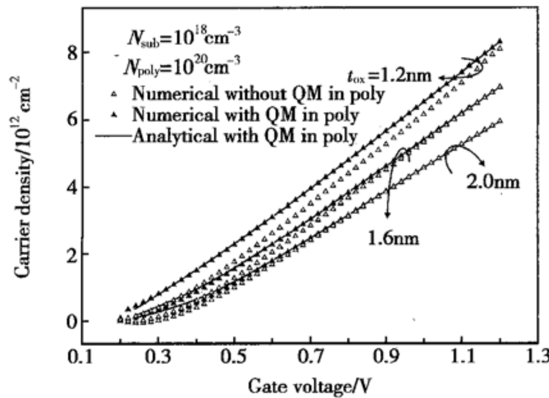


Fig. 7 Carrier density, with $N_{poly}=10^{20}cm^{-3}$, $N_{sub}=10^{18}cm^{-3}$, and different oxide thickness ($t_{ox}$ = 1.2nm, $t_{ox}$ = 1.6nm, and $t_{ox}$ = 2.0nm) Solid symbols represent numerical results with QM in the poly-gate and hollow symbols represent those without QM in the poly-gate. Solid lines stand for analytical results with QM in the poly-gate.

## 5 Conclusion

In this paper, a newly developed approach, the GCS approach, is presented for compact modeling of the new physical effects in nanoscale MOSFETs. Subsequently, it is applied to develop a compact model for the QM effects in poly-gates on the basis of the DG formulation. It is concluded that the QM effects are non-negligible in nanoscale MOSFETs and have an opposite influence on the device characteristics as the PD effects do.

## References

[1] Hou Yongtian, Li Mingfu, Jin Ying. Direct tunneling currents through gate dielectrics in deep submicron MOSFETs. Chinese Journal of Semiconductors, 2002, 23(5): 449

[2] Ma Yutao, Li Zhijian, Liu Litian. MOS device threshold voltage model considering quantum mechanical effect including multi-subband occupation. Chinese Journal of Semiconductors, 1999, 20(3): 219(in Chinese) [马玉涛, 李志坚, 刘理天. 包含多子带结构的MOS器件开启电压量子力学效应修正模型. 半导体学报, 1999, 20(3): 219]

[3] Pirovano A, Lacaita A L, Spinelli A S. Two-dimensional quantum effects in nanoscale MOSFETs. IEEE Trans Electron Devices, 2002, 49(1): 25

[4] http://www-device.eecs.berkeley.edu/~bsim3/BSIM4

[5] Yu Z, Yergeau D W, Dutton R W, et al. Quantum transport model for sub-100nm CMOS devices. Proc SPIE, 2001, 4600: 117

[6] Yu Z, Dutton R W, Yergeau D, et al. Macroscopic carrier transport modeling. SISPAD'01, 2001

[7] http://www.synopsys.com/products/acmgr/ise/former_ise_overview.html

## Appendix A

In this appendix, the extensive explanation is made for numerical simulations throughout our work that are executed by the software DESSIS in ISE 8.0. Simulation regions include the three regions of a MOS structure, i.e. poly-gate, gate-oxide, and substrate. The five partial-differential-equation (PDE) set implemented is shown as follows including Poisson equation (A1), continuity equations (A2, A3). and equations from Boltzmann statistics (A4, A5)

$$\nabla(\epsilon\nabla\psi)+q(p-n+N_D^+-N_A^-)=0 \quad (A1)$$

$$\nabla(\mu_n n\nabla\phi_n)+\frac{\partial n}{\partial t}+r=0 \quad (A2)$$

$$\nabla(\mu_p p\nabla\phi_p)-\frac{\partial p}{\partial t}-r=0 \quad (A3)$$

$$\psi-\frac{k_BT}{q}\ln\frac{n}{n_i}-\phi_n+\Delta\psi_{QM,n}=0 \quad (A4)$$

$$\psi-\frac{k_BT}{q}\ln\frac{p}{n_i}-\phi_p+\Delta\psi_{QM,p}=0 \quad (A5)$$

with quantum potentials $\Delta\psi_{QM,n}=\frac{2}{\sqrt{n}}\times\nabla\times\left[\frac{\hbar^2}{4lqm_n^*}\times\nabla\sqrt{n}\right]$ and $\Delta\psi_{QM,p}=\frac{2}{\sqrt{p}}\times\nabla\times\left[\frac{\hbar^2}{4lqm_p^*}\times\nabla\sqrt{p}\right]$. Before the boundary conditions for quantum potentials are discussed, the smoothed potential (take electrons as example) $\bar{\phi}=E_C/q-\frac{k_BT}{q}\times\ln\frac{N_C}{N_{ref}}-\Delta\psi_{QM,n}$ (with the conduction band energy $E_C$, the conduction band edge density of states $N_C$, and an arbitrary normalization constant $N_{ref}$) is introduced. With it, the quantum

potential can be rewritten as:

$$\Delta\Psi_{QM,n} = \frac{\hbar^2}{4lm_n^*}\left[\nabla\times q/k_BT(\nabla\phi_n - \nabla\bar{\phi}) + q^2/2k_B^2T^2(\nabla\phi_n - \nabla\bar{\phi})^2\right] \quad (A6)$$

At ohmic contacts, resistive contacts and current contacts, the boundary condition $\Delta\Psi_{QM,n(p)} = 0$ is imposed. At all other contacts and external boundaries homogeneous Neumann boundary conditions are used, $\hat{n}[q/k_BT(\nabla\phi_n - \nabla\bar{\phi})] = 0$, with $\hat{n}$ normal vector on the boundary. At internal interfaces, $\bar{\phi}$ and $\hat{n}[q/k_BT(\nabla\phi_n - \nabla\bar{\phi})]$ must be continuous.

## Appendix B

In this appendix, the deduction from Eqs. (5) and (6) in the main text to Eq. (7) is presented. From Eq. (6), the quantum potential in 1-D case can be expressed as:

$$\Delta\Psi_{QM} = -\frac{\hbar^2}{4lqm_n^*}\left[\left(\frac{\partial n}{\partial x}\right)^2\times\frac{1}{2n^2} - \frac{\partial^2 n}{\partial x^2}\times\frac{1}{n}\right] \quad (B1)$$

On the other hand, from Eq. (5) the derivatives of $n$ are deduced as follows:

$$\frac{\partial n}{\partial x} = \frac{qn}{k_BT}\left(\frac{\partial\Psi}{\partial x} + \frac{\partial\Delta\Psi_{QM}}{\partial x}\right) \quad (B2)$$

$$\frac{\partial^2 n}{\partial x^2} = \frac{qn}{k_BT}\times\left[\frac{q}{k_BT}\times\left(\frac{\partial\Psi}{\partial x} + \frac{\partial\Delta\Psi_{QM}}{\partial x}\right)^2 + \left(\frac{\partial^2\Psi}{\partial x^2} + \frac{\partial^2\Delta\Psi_{QM}}{\partial x^2}\right)\right] \quad (B3)$$

Substituting Eqs. (B2) and (B3) into (B1), the following equation is obtained:

$$\frac{\hbar^2}{4lm_n^*k_BT}\times\frac{\partial^2\Delta\Psi_{QM}}{\partial x^2} + \left(\frac{\hbar^2 q}{4lm_n^*k_B^2T^2}\times\frac{\partial\Psi}{\partial x}\right)\times\frac{\partial\Delta\Psi_{QM}}{\partial x} - \Delta\Psi_{QM} + \left[\frac{\hbar^2 q}{8lm_n^*k_B^2T^2}\times\left(\frac{\partial\Psi}{\partial x}\right)^2 + \frac{\hbar^2}{4lm_n^*k_BT}\times\frac{\partial^2\Psi}{\partial x^2}\right] = 0 \quad (B4)$$

This is Eq. (7) in the main text and therefore the deduction is finished.

# GCS 法及多晶区量子效应的集约建模*

张大伟[1]　章　浩[2]　田立林[1]　余志平[1]

(1 清华大学微电子学研究所, 北京　100084)

(2 清华大学电子工程系, 北京　100084)

**摘要**: 提出了一种新的建立集约模型的方法, 即栅电容修正法. 此方法考虑了新型效应对栅电压的依赖关系, 且可以对各种效应相对独立地建模并分别嵌入模型中. 另外, 利用该方法和密度梯度模型建立了一个多晶区内量子效应的集约模型. 该模型与数值模拟结果吻合. 模型结果和模拟结果均表明, 多晶区内的量子效应不可忽略, 且它对器件特性的影响与多晶耗尽效应相反.

**关键词**: 集约模型; 纳米级; 栅电容修正法; 多晶区内的量子力学效应

**PACC**: 7340Q; 6185; 0300

**中图分类号**: TN304.02　　**文献标识码**: A　　**文章编号**: 0253-4177(2004)12-1599-07

* 国家高技术研究发展计划资助项目(批准号: 2003AA1Z1370)

张大伟　男, 1980 年出生, 硕士研究生, 主要从事纳米级器件中新型物理效应的集约解析建模.

章　浩　男, 1983 年出生, 大学本科生, 主要从事亚 100nm MOSFET 中量子力学效应的解析建模.

2004-02-18 收到, 2004-07-05 定稿

©2004 中国电子学会